Journal of Coordination Chemistry

ISSN: 0095-8972 (Print) 1029-0389 (Online) Journal homepage: http://www.tandfonline.com/loi/gcoo20

Synthesis, crystal structures and electrocatalytic properties of bridgehead-C-functionalized diiron dithiolate complexes

Pei-Hua Zhao, Kuan-Kuan Xiong, Wen-Jun Liang & Er-Jun Hao

To cite this article: Pei-Hua Zhao, Kuan-Kuan Xiong, Wen-Jun Liang & Er-Jun Hao (2015) Synthesis, crystal structures and electrocatalytic properties of bridgehead-C-functionalized diiron dithiolate complexes, Journal of Coordination Chemistry, 68:6, 968-979, DOI: 10.1080/00958972.2014.1002398

To link to this article: http://dx.doi.org/10.1080/00958972.2014.1002398

Accepted author version posted online: 24 Dec 2014.
Published online: 07 Jan 2015.

Journal of Coordination Chemistry, 2015
Vol. 68, No. 6, 968–979, http://dx.doi.org/10.1080/00958972.2014.1002398

Synthesis, crystal structures and electrocatalytic properties of bridgehead-C-functionalized diiron dithiolate complexes

PEI-HUA ZHAO*†, KUAN-KUAN XIONG†, WEN-JUN LIANG† and ER-JUN HAO*‡

†Research Center for Engineering Technology of Polymeric Composites of Shanxi Province, School of Materials Science and Engineering, North University of China, Taiyuan, PR China
‡School of Chemistry and Chemical Engineering, Henan Normal University, Xinxiang, PR China

(*Received 24 August 2014; accepted 12 December 2014*)

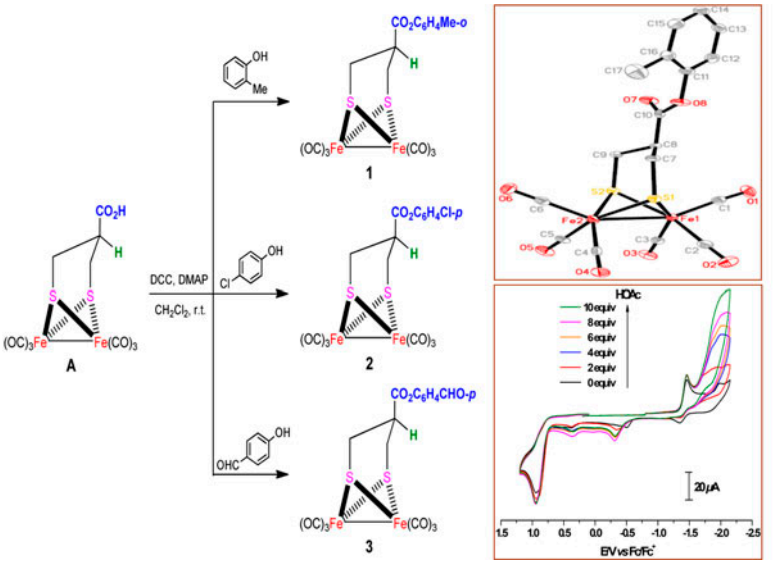

To investigate the influence of bridgehead-C functionality in diiron dithiolate complexes on the molecular structure and electrocatalytic properties of [FeFe]-hydrogenase models, three new bridgehead-C-functionalized model complexes **1–3** have been synthesized and structurally characterized. Treatments of parent complex $[(\mu\text{-}SCH_2)_2CHCO_2H][Fe_2(CO)_6]$ (**A**) with the esterification agents *o*-MeC_6H_4OH, *p*-ClC_6H_4OH, or *p*-HOC_6H_4CHO in the presence of 4-dimethylaminopyridine and dicyclohexylcarbodiimide in CH_2Cl_2 at room temperature resulted in formation of $[(\mu\text{-}SCH_2)_2CHCO_2R][Fe_2(CO)_6]$ (*R* = *o*-MeC_6H_4–, **1**; *p*-ClC_6H_4–, **2**; *p*-$OHCC_6H_4$–, **3**) in 53–55% yields. The new complexes **1–3** were characterized by elemental analysis, IR and NMR spectroscopy, and especially determined by X-ray crystallography. The electrochemical properties of **1–3** and the electrocatalytic H_2 evolution catalyzed by **1** have been investigated by cyclic voltammetry, where **1** is a catalyst for HOAc proton reduction to H_2 under electrochemical conditions.

*Corresponding authors. Email: zph2004@nuc.edu.cn (P.-H. Zhao); erjunh@163.com (E.-J. Hao)

Keywords: Diiron dithiolate complexes; Bridgehead-C-functionalized; Synthesis; Crystal structure; Electrocatalytic property

1. Introduction

Diiron dithiolate complexes have attracted attention because their unique [2Fe2S] butterfly structures are biologically related to the active site of [FeFe]-hydrogenase, which has extremely high catalytic ability for the production of renewable hydrogen fuel [1, 2]. X-ray crystallographic and theoretical investigations have revealed that: (i) the active site of [FeFe]-hydrogenase is composed of a butterfly [2Fe2S] cluster linked to a cubic [4Fe4S] cluster via sulfur of a cysteinyl moiety [3, 4]; (ii) in the active site, the two iron centers in the butterfly cluster are bridged by dithiolate and coordinated by CO/CN^- ligands, where the bridging dithiolate may be assigned as a propanedithiolate (PDT, $SCH_2CH_2CH_2S$) [4, 5] or azadithiolate (ADT, SCH_2NCH_2S) [6, 7]; (iii) the [2Fe2S] cluster serves as the catalytic center for proton reduction, and the [4Fe4S] cluster mediates electron transfer to and from the active site [8]. The above-mentioned structural information has inspired chemists to synthesize a large number of biomimetic models [9–16], in which the bridgehead-C-substituted diiron dithiolate model complexes are of particular interest as they can be easily obtained by functional transformation reactions and display catalytic properties [17–23]. However, it is worthy of note that although parent complex [(μ-SCH_2)$_2$$CHCO_2H$][$Fe_2(CO)_6$] (**A**) has been prepared by Darensbourg and co-workers [18], there are only a few derivatives synthesized from it [18, 24], and particularly the comparative study on the catalytic behavior of its derivatives is not reported.

As a continuation of our project concerning the biomimetic chemistry of [FeFe]-hydrogenase [24–30] and to investigate the influence of bridgehead-C functionality in diiron dithiolate model complexes toward their molecular structures and electrocatalytic properties, we herein report the synthesis, crystal structures, and electrocatalytic properties of **1–3** derived from their parent complex (**A**).

2. Experimental

2.1. *Materials and methods*

All reactions and operations were carried out under a dry, oxygen-free nitrogen atmosphere with standard Schlenk and vacuum-line techniques. CH_2Cl_2 was distilled with CaH_2 under N_2. Dicyclohexylcarbodiimide (DCC), N,N-dimethylaminopyridine (DMAP), *o*-MeC_6H_4OH, and *p*-ClC_6H_4OH, *p*-HOC_6H_4CHO, and other materials were commercially available and used as received. [(μ-SCH_2)$_2$$CHCO_2H$][$Fe_2(CO)_6$] (**A**) was prepared according to the literature [18]. Preparative TLC was carried out on glass plates (25 cm × 20 cm × 0.25 cm) coated with silica gel H (10–40 mm). IR spectra were recorded on a Nicolet 670 FTIR spectrometer. ^1H (^{13}C) NMR spectra were obtained on a Bruker Avance 400 MHz spectrometer. Elemental analyses were performed on a Perkin-Elmer 240C analyzer. Melting points were determined on a YRT-3 apparatus and are uncorrected.

2.2. *Synthesis of [(μ-SCH_2)$_2$$CHCO_2C_6H_4$Me-o][$Fe_2(CO)_6$] (1)*

A CH_2Cl_2 (15 mL) solution of [(μ-SCH_2)$_2$$CHCO_2H$][$Fe_2(CO)_6$] (0.215 g, 0.5 mM), DCC (0.124 g, 0.6 mM), and DMAP (0.013 g, 0.1 mM) was stirred at room temperature for

5 min. To the above mixture, *o*-MeC_6H_4OH (0.062 mL, 0.6 mM) was added, and the reaction mixture was stirred at room temperature for 12 h. The solvent was removed on a rotary evaporator and the residue was subjected to preparative TLC separation using CH_2Cl_2/petroleum ether (v/v = 1 : 2) as eluent. From the main red band, **1** (0.144 g, 55%) was obtained as a red solid. M.p.: 130–131 °C. Anal. Calcd for $C_{17}H_{12}Fe_2O_8S_2$ (%): C, 39.26; H, 2.33. Found (%): C, 39.21; H, 2.45. IR (KBr disk, cm^{-1}): $\nu_{C\equiv O}$ 2073 (vs), 2034 (vs), 2005 (vs), 1993 (vs), 1972 (vs); $\nu_{C(O)O}$ 1749 (s). ^{1}H NMR (400 MHz, $CDCl_3$, TMS, ppm): 7.20 (m, 3H, Ph*H*), 6.92 (d, *J* = 7.2 Hz, 1H, Ph*H*), 3.05 (dd, *J* = 13.6, 2.8 Hz, 2H, $2SCH_aH_e$), 2.39 (t, *J* = 13.6 Hz, 1H, C*H*), 2.10 (s, 3H, CH_3), 1.87 (t, *J* = 13.6 Hz, 2H, $2SCH_aH_e$). ^{13}C NMR (100.6 MHz, $CDCl_3$, TMS, ppm): 207.40, 207.05 (Fe*C*O), 169.29 (*C*(O)O), 148.69 (Ph*C*O), 131.35, 127.14, 126.56, 121.45 (Ph*C*H), 129.59 (Ph*C*Me), 48.33 (*C*H), 24.86 (SCH_2), 16.19 (CH_3) (Note: H_a and H_e denote the axially and equatorially bonded hydrogens in CH_2S groups in this article).

2.3. *Synthesis of [(μ-SCH_2)$_2$$CHCO_2C_6H_4$Cl-p][$Fe_2(CO)_6$] (2)*

The procedure was similar to that of **1** except *p*-ClC_6H_4OH (0.059 mL, 0.6 mM) was used instead of *o*-MeC_6H_4OH (0.062 mL, 0.6 mM). Complex **2** (0.150 g, 55%) was obtained as a red solid. M.p.: 165–166 °C. Anal. Calcd for $C_{16}H_9ClFe_2O_8S_2$ (%): C, 35.55; H, 1.68. Found (%): C, 35.50; H, 1.85. IR (KBr disk, cm^{-1}): $\nu_{C\equiv O}$ 2074 (vs), 2032 (vs), 2007 (vs), 1988 (vs), 1981 (vs); $\nu_{C(O)O}$ 1750 (s). ^{1}H NMR (400 MHz, $CDCl_3$, TMS, ppm): 7.33 (d, *J* = 7.2 Hz, 2H, Ph*H*), 6.97 (d, *J* = 7.2 Hz, 2H, Ph*H*), 3.01 (d, *J* = 13.6 Hz, 2H, $2SCH_aH_e$), 2.35 (t, *J* = 13.6 Hz, 1H, C*H*), 1.83 (t, *J* = 13.6 Hz, 2H, $2SCH_aH_e$). ^{13}C NMR (100.6 MHz, $CDCl_3$, TMS, ppm): 207.34, 206.99 (Fe*C*O), 169.38 (*C*(O)O), 148.54 (Ph*C*O), 131.82 (Ph*C*Cl), 129.67, 122.52 (Ph*C*H), 48.20 (*C*H), 24.69 (SCH_2).

2.4. *Synthesis of [(μ-SCH_2)$_2$$CHCO_2C_6H_4$CHO-p][$Fe_2(CO)_6$] (3)*

The procedure was similar to that of **1** except *p*-HOC_6H_4CHO (0.073 g, 0.6 mM) was used instead of *o*-MeC_6H_4OH (0.062 mL, 0.6 mM). Complex **3** (0.141 g, 53%) was obtained as a red solid. M.p.: 138–139 °C. Anal. Calcd for $C_{17}H_{10}ClFe_2O_9S_2$ (%): C, 38.23; H, 1.89. Found (%): C, 38.21; H, 1.99%. IR (KBr disk, cm^{-1}): $\nu_{C\equiv O}$ 2069 (vs), 2033 (vs), 2006 (vs), 1989 (vs), 1973 (vs), 1964 (vs); $\nu_{C(O)O}$ 1744 (s); ν_{CHO} 1695 (s). ^{1}H NMR (400 MHz, $CDCl_3$, TMS, ppm): 9.98 (s, 1H, C*H*O), 7.90 (d, *J* = 8.4 Hz, 2H, Ph*H*), 7.20 (d, *J* = 8.4 Hz, 2H, Ph*H*), 3.01 (dd, *J* = 13.6, 3.6 Hz, 2H, $2SCH_aH_e$), 2.37 (t, *J* = 13.6 Hz, 1H, C*H*), 1.84 (t, *J* = 13.6 Hz, 2H, $2SCH_aH_e$). ^{13}C NMR (100.6 MHz, $CDCl_3$, TMS, ppm): 207.40, 207.05 (Fe*C*O), 190.79 (*C*HO), 169.04 (*C*(O)O), 154.74 (Ph*C*O), 134.48 (Ph*C*CHO), 131.40, 122.14 (Ph*C*H), 48.32 (*C*H), 24.71 (SCH_2).

2.5. *X-ray structure determination*

Single crystals of **1–3** suitable for X-ray diffraction analysis were grown by slow evaporation of the CH_2Cl_2/hexane solution at 5 °C. Single crystals of **1–3** were mounted on a Rigaku MM-007 CCD diffractometer. Data were collected at 113(2) K for **1**, **3** and for 293 (2) K for **2** by using a graphite monochromator with Mo-Kα radiation (λ = 0.71073 Å) in the $\omega - \varphi$ scanning mode. Data collection, reduction, and absorption correction were performed by the CRYSTALCLEAR program [31]. The structure was solved by direct

methods using SHELXS-97 [32] and refined by full-matrix least-squares (SHELXL-97) [33] on F^2. Hydrogens were located using the geometric method.

2.6. *Electrochemistry*

Electrochemical measurements were carried out using a CHI 620 Electrochemical Workstation (CH Instruments, Chenhua, Shanghai, China). A solution of 0.1 M *n*-Bu_4NPF_6 in CH_3CN was used as the electrolyte and was degassed by bubbling with dry nitrogen for 10 min before measurement. Cyclic voltammograms (CVs) were obtained in a three-electrode cell with a glassy carbon electrode (3 mm diameter) as the working electrode, successively polished with 3 and 1 μm diamond pastes and sonicated in ion-free water for 10 min, a platinum wire as the counter electrode, and a non-aqueous Ag/Ag^+ electrode (1.0 mM $AgNO_3$ and 0.1 M *n*-Bu_4NPF_6 in CH_3CN) as the reference electrode. The potential scale was calibrated against the Fc/Fc^+ couple and reported *versus* this reference system.

3. Results and discussion

3.1. *Synthesis and characterization of 1–3*

As displayed in scheme 1, reactions of $[(\mu\text{-}SCH_2)_2CHCO_2H][Fe_2(CO)_6]$ (**A**) with 1.2 equiv. of *o*-MeC_6H_4OH, *p*-ClC_6H_4OH, or *p*-HOC_6H_4CHO in the presence of the dehydrating reagent DCC and the catalyst DMAP in CH_2Cl_2 at room temperature afforded the expected diiron dithiolate complexes $[(\mu\text{-}SCH_2)_2CHCO_2R][Fe_2(CO)_6]$ (R = *o*-MeC_6H_4–, **1**; *p*-ClC_6H_4–, **2**; *p*-$OHCC_6H_4$–, **3**) in moderate yields.

The model complexes **1–3** were air-stable red solids, which have been fully characterized by elemental analysis, IR, and ^1H (^{13}C) NMR spectroscopic techniques. The results of the elemental analyses for **1–3** are in agreement with the corresponding compositions (as shown in the Experimental section). The IR spectra of **1–3** in KBr display five or six strong absorptions from 2074 to 1964 cm^{-1} for their terminal carbonyls, whereas that of **3** shows one additional absorption at 1695 cm^{-1} for its aldehyde carbonyl. The distinct difference in the IR data of **1–3** with **A** is the disappearance of the band at 1730 cm^{-1} for **A** [18] and the appearance of a new band at 1750 cm^{-1} for **1–3**, demonstrating that the carboxyl group in **A** is changed into the ester groups in **1–3**. Meanwhile, the frequency value of the highest CO stretching bands in the FT-IR spectrum is usually a useful indicator for detecting variation in the electron density of Fe in diiron dithiolate complexes and further evaluating the coordination geometry of Fe attached to CO. The values of the highest ν(CO) bands for **1–3** (ca. 2073 cm^{-1}) are very similar to those of their parent complex (**A**) and other all-carbonyl diiron dithiolate complexes [14–24], but are obviously more than those of most substituted-carbonyl diiron complexes [25, 34–36]. This indicated that the bridgehead-C functionality of **1–3** has almost no effect on the electron density and coordination geometries of Fe ions in diiron dithiolate complexes.

The ^1H NMR spectra of **1–3** give a doublet of doublets or doublet at ca. 3.05 ppm and two triplets at ca. 2.39 as well as 1.87 ppm for their $(SCH_2)_2CH$ groups. The ^1H NMR spectra of **1–3** show two types of aromatic proton signals at 7.90–6.92 ppm for their phenyl moieties. Moreover, the ^1H NMR spectra of **1** and **3** display sharp singlets at 2.10 and 9.98 ppm for the methyl and aldehyde group, respectively. In addition, the ^{13}C NMR

Table 1. Crystal data and structural refinements details for **1–3**.

Complex	**1**	**2**	**3**
Empirical formula	$C_{17}H_{12}Fe_2O_8S_2$	$C_{16}H_9ClFe_2O_8S_2$	$C_{17}H_{10}Fe_2O_9S_2$
Formula weight	520.09	540.50	534.07
Temperature (K)	113(2)	293(2)	293(2)
Wavelength (Å)	0.71073	0.71073	0.71073
Crystal system	Triclinic	Monoclinic	Monoclinic
Space group	*P-1*	*P2(1)/n*	*P2(1)/n*
a (Å)	8.968(10)	10.0708(4)	10.104(2)
b (Å)	9.016(10)	17.4210(9)	17.669(4)
c (Å)	12.894(15)	11.5883(5)	11.422(2)
α (°)	95.277(14)	90	90
β (°)	108.06(2)	97.163(4)	96.32(3)
γ (°)	95.442(14)	90	90
V (Å^3)	978.6(19)	2017.23(16)	2026.7(7)
Z	2	4	4
D_{Calcd} (g cm^{-3})	1.765	1.780	1.750
μ (mm^{-1})	1.739	1.819	1.685
F(0 0 0)	524	1080	1072
Crystal size (mm)	0.20 × 0.18 × 0.12	0.30 × 0.28 × 0.20	0.20 × 0.18 × 0.14
θ_{min}, θ_{max} (°)	1.68, 25.02	2.93, 26.37	2.13, 27.97
Reflections collected/unique	8059/3440	9954/4120	20,525/4844
R_{int}	0.0389	0.0428	0.0485
hkl range	$-9 \le h \le 10$	$-12 \le h \le 12$	$-13 \le h \le 13$
	$-10 \le k \le 10$	$-11 \le k \le 21$	$-23 \le k \le 20$
	$-15 \le l \le 15$	$-14 \le l \le 14$	$-15 \le l \le 15$
Completeness to θ_{max} (%)	99.5	99.8	99.3
Data/restraints/parameters	3440/0/263	4120/0/262	4844/0/272
Goodness-of-fit (GOF) on F^2	0.914	1.018	0.992
R_1/wR_2 [$I>2\sigma(I)$]	0.0275/0.0385	0.0436/0.0699	0.0364/0.0724
R_1/wR_2 (all data)	0.0328/0.0393	0.0779/0.0823	0.0538/0.0820
Largest difference peak/hole (e A^{-3})	0.381/−0.386	0.450/−0.334	0.462/−0.396

Table 2. Selected bond lengths (Å) and angles (°) for **1–3**.

Complex	**1**	**2**	**3**
Fe(1)–Fe(2)	2.5014(18)	2.5028(8)	2.5072(6)
Fe(1)–S(2)	2.271(2)	2.2553(10)	2.2551(8)
Fe(1)–S(1)	2.273(2)	2.2551(11)	2.2623(7)
Fe(2)–S(2)	2.251(2)	2.2481(11)	2.2494(8)
Fe(2)–S(1)	2.263(2)	2.2458(10)	2.2494(8)
Fe(1)–C(3)	1.788(3)	1.788(4)	1.793(3)
Fe(1)–C(2)	1.797(3)	1.802(4)	1.785(3)
Fe(1)–C(1)	1.808(3)	1.780(4)	1.808(3)
Fe(2)–C(6)	1.800(3)	1.792(4)	1.802(3)
Fe(2)–C(5)	1.805(3)	1.794(5)	1.800(3)
Fe(2)–C(4)	1.813(3)	1.792(4)	1.783(3)
O(7)–C(10)	1.191(3)	1.175(4)	1.172(3)
O(8)–C(10)	1.370(3)	1.336(4)	1.352(3)
S(2)–Fe(1)–S(1)	84.42(7)	84.67(4)	84.41(3)
S(2)–Fe(1)–Fe(2)	56.04(6)	56.10(3)	56.08(2)
S(1)–Fe(1)–Fe(2)	56.35(5)	56.04(3)	55.99(2)
S(2)–Fe(2)–S(1)	85.10(6)	85.06(4)	84.83(3)
S(2)–Fe(2)–Fe(1)	56.81(6)	56.38(3)	56.28(2)
S(1)–Fe(2)–Fe(1)	56.71(6)	56.39(3)	56.485(17)
Fe(2)–S(1)–Fe(1)	66.94(5)	67.57(3)	67.52(2)
Fe(2)–S(2)–Fe(1)	67.15(3)	67.52(3)	67.64(2)

spectra of **1–3** show two downfield carbon signals at 207.40 and 207.05 ppm for the iron carbonyls, while **3** demonstrates one typical carbon signal at 190.79 ppm for its aldehyde carbonyl. Especially, one characteristic ester carbon signal at ca. 169.29 cm^{-1} is observed in the ^{13}C NMR spectra of **1–3**, indicating that the carboxyl group of **A** has been transformed into the ester moiety of **1–3** via condensation.

3.2. *X-ray crystal structures of 1–3*

The molecular structures of **1–3** have been unequivocally confirmed by X-ray crystallography. The ORTEP views of **1–3** are illustrated in figures 1–3. A summary of cell parameters,

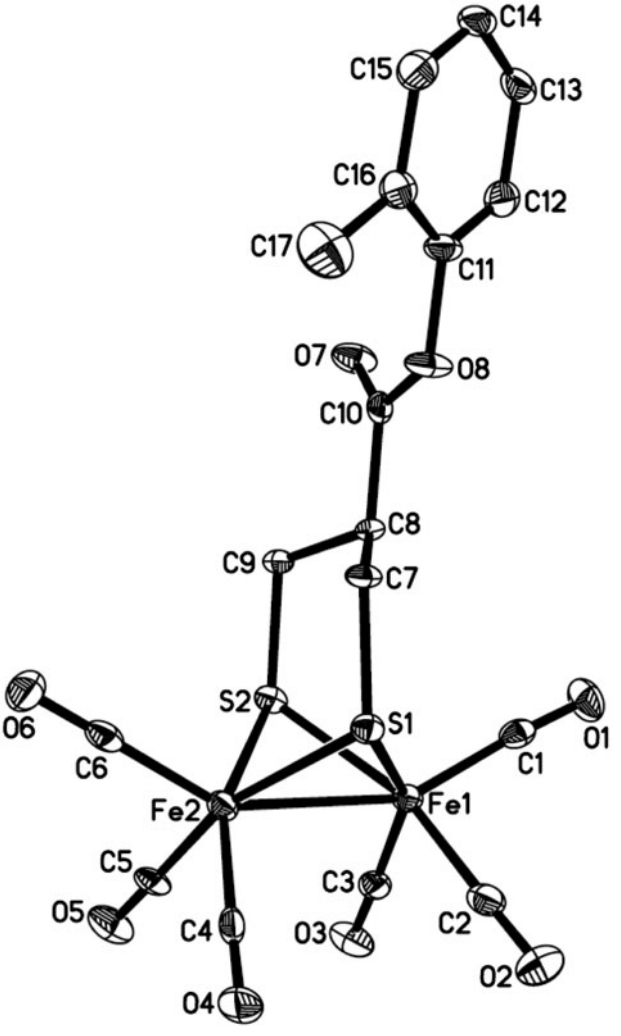

Figure 1. Molecular structure of **1** with thermal ellipsoids at 30% probability.

data collection, and structure refinement is listed in table 1. Selected bond lengths and angles are given in table 2.

As shown in figures 1–3, **1–3** consist of a butterfly [2Fe2S] cluster core coordinated by six carbonyl ligands and bridged by one PDT unit, where the ester moiety is attached to the bridgehead C8 via the sterically favored equatorial bond. The diiron PDT unit contains two fused six-membered FeS_2C_3 rings including the chair-shaped C8C9S2Fe2S1C7 and the boat-shaped C8C9S2Fe1S1C7. Such molecular features of **1–3** are in accord with those reported in the bridgehead-C-functionalized diiron dithiolate model complexes [(μ-$SCH_2)_2CHR$][$Fe_2(CO)_6$] (R = –CO_2H [37], –$C(O)NHC_6H_5$ [18], –$CO_2CH_2CH_2Cl$ [24], –$CO_2C_6H_4I$-p [24], –OH [19], –$O_2CC_6H_5$ [19], –$O_2CC_4H_3O$-2 [19], –$O_2CC_4H_3S$-2 [19],

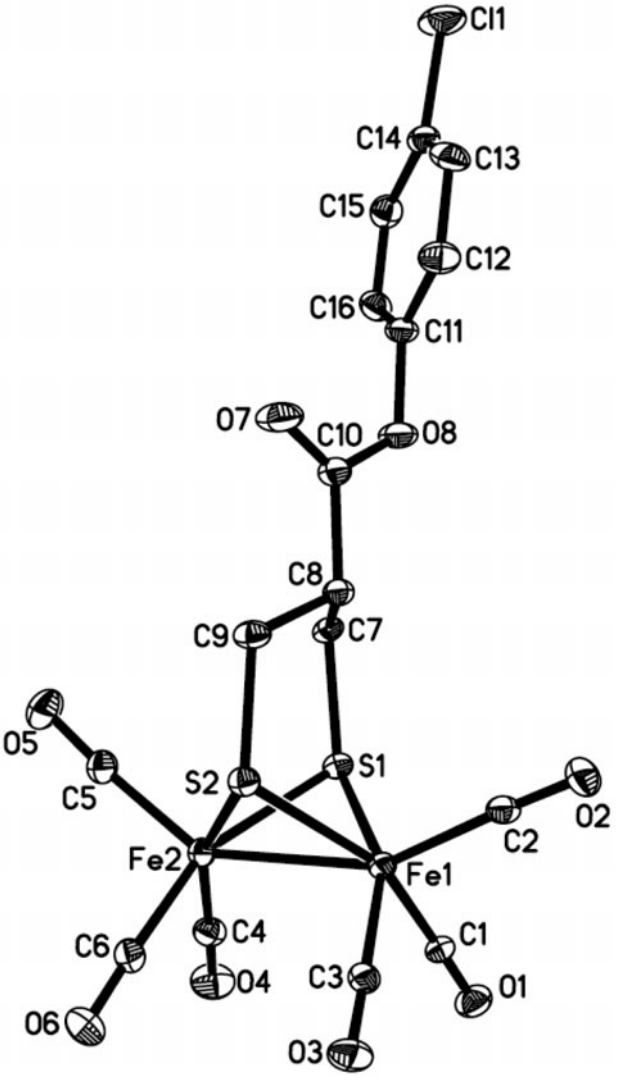

Figure 2. Molecular structure of **2** with thermal ellipsoids at 30% probability.

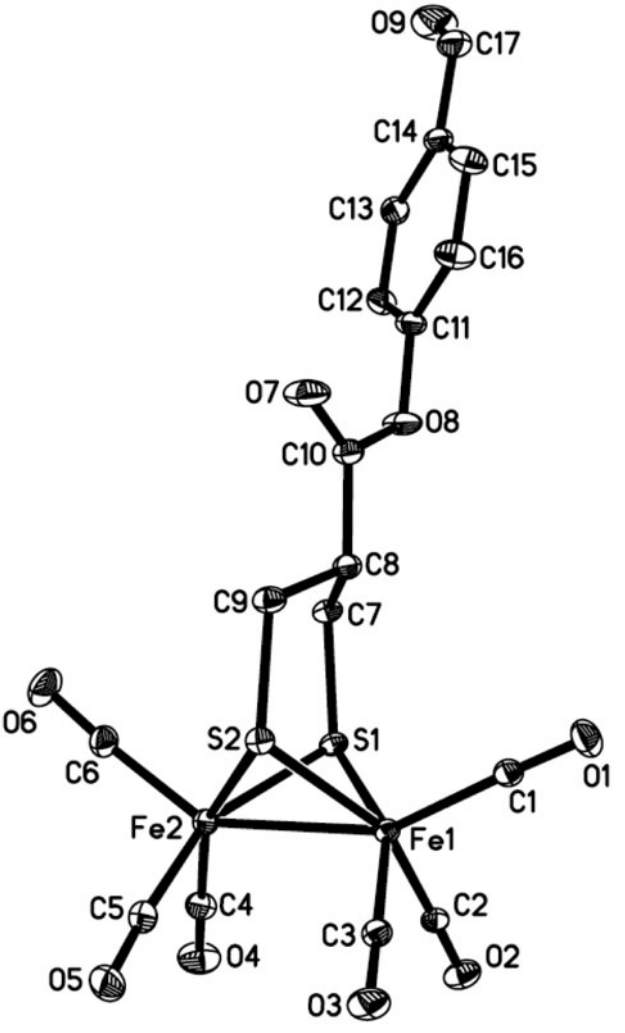

Figure 3. Molecular structure of **3** with thermal ellipsoids at 30% probability.

–$O_2CCH_2CO_2Et$ [20], –$O_2CC_6H_4NHBoc$-*p* [17], –$O_2CC_6H_4NHBoc$-*p* [17], and –Ph [23]). These indicate that the bridgehead-C functionality in diiron dithiolate model complexes has almost no effect on the molecular geometry of **1–3**.

The Fe–Fe distances in **1** (2.5014(18) Å), **2** (2.5028(8) Å), and **3** (2.5072(6) Å) are slightly shorter than that of **A** (2.513 Å) [34], but are sharply shorter than those found in the natural [FeFe]-hydrogenase isolated from enzymes *Clostridium pasteurianum* and *Desulfovibrio desulfuricans* (2.55–2.62 Å) [3, 4]. Particularly noteworthy is that the dihedral angle between the ester group [the O7C10O8 plane for **1–3** and the phenyl moiety [the C11–C16 plane for **1–3** (derivation 0.0052, 0.0056, and 0.0038 Å)] is 124.6°, 118.3°, and 57.7°, respectively, demonstrating that the bridgehead-C substituent is not coplanar in crystal structures of **1–3**.

Table 3. Electrochemical data of **1**–**3**.

Complex	E_{pa1} (V)	E_{pa2} (V)	E_{pc1} (V)	E_{pc2} (V)
1	–	+0.941	−1.461	−1.987
2	+0.872	+0.958	−1.456	−1.963
3	–	+0.963	−1.456	−1.963

3.3. *Electrochemistry of 1–3*

In order to study the effect of bridgehead-C functionality in PDT on the electrochemical properties of diiron dithiolate model complexes, the redox properties of **1–3** have been investigated by cyclic voltammetry in MeCN under N_2. The electrochemical data of **1–3** are listed in table 3, whereas the corresponding CVs are displayed in figure 4. The model complexes **1–3** show one quasi-reversible reduction, one irreversible reduction, and one or two irreversible oxidations. With reference to the previous assignments for electrochemical reduction potentials of parent complex $[(\mu\text{-}SCH_2)_2CHCO_2H][Fe_2(CO)_6]$ (**A**) [18], the first quasi-reversible reduction peaks at −1.461 V for **1**, −1.456 V for **2**, and −1.456 V for **3** may be attributed to the $[Fe^IFe^I] + e^- \rightarrow [Fe^IFe^0]$ one-electron reduction, whilst the second irreversible reduction peaks at −1.987 V for **1**, −1.963 V for **2**, and −1.963 V for **3** should be assigned to the $[Fe^IFe^0] + e^- \rightarrow [Fe^0Fe^0]$ one-electron reduction process. The cyclic voltammetric behaviors of **1–3** are very similar to one another, demonstrating that the bridgehead-C functionality has little impact on the electrochemical reduction properties of **1–3**.

To further investigate the electrocatalytic H_2 production activity of such model complexes, the electrochemically catalytic proton reduction by **1** has been studied in the presence of weak acid HOAc. As displayed in figure 5, upon addition of 2 mM HOAc to the MeCN solution of **1**, the height of the first reduction peak of **1** at −1.459 V increases slightly and ceases to grow with sequential increments of acid concentration. However, in contrast to this, the height of the second reduction peak at −1.979 V shows a linear increase dependent on the concentration of HOAc. Such observation indicates an electrocatalytic proton reduction process [38–40]. This has indicated that **1** is active for the electrocatalytic H_2 evolution in the presence of HOAc.

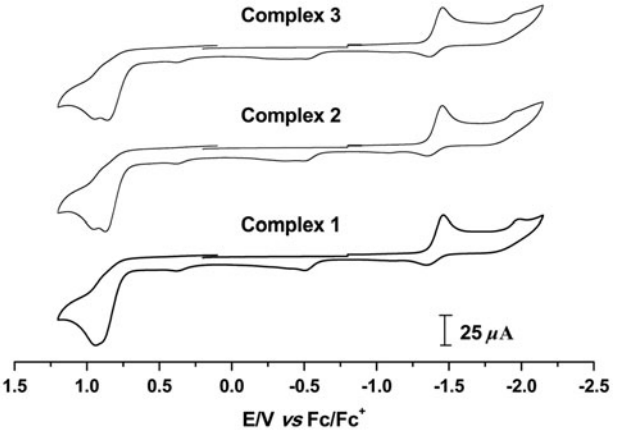

Figure 4. CVs of **1–3** (1.0 mM) in 0.1 M n-Bu_4NF_6/MeCN at a scan rate of 100 mV/s.

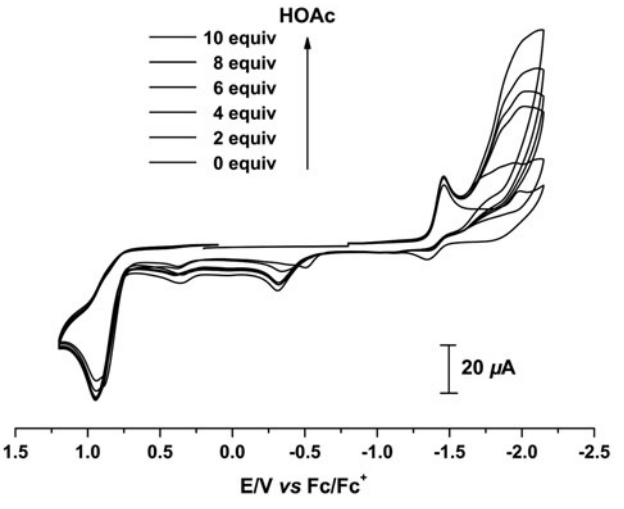

Figure 5. CV of **1** (1.0 mM) with HOAc (0–10 mM) in 0.1 M n-Bu_4NF_6/MeCN at a scan rate of 100 mV/s.

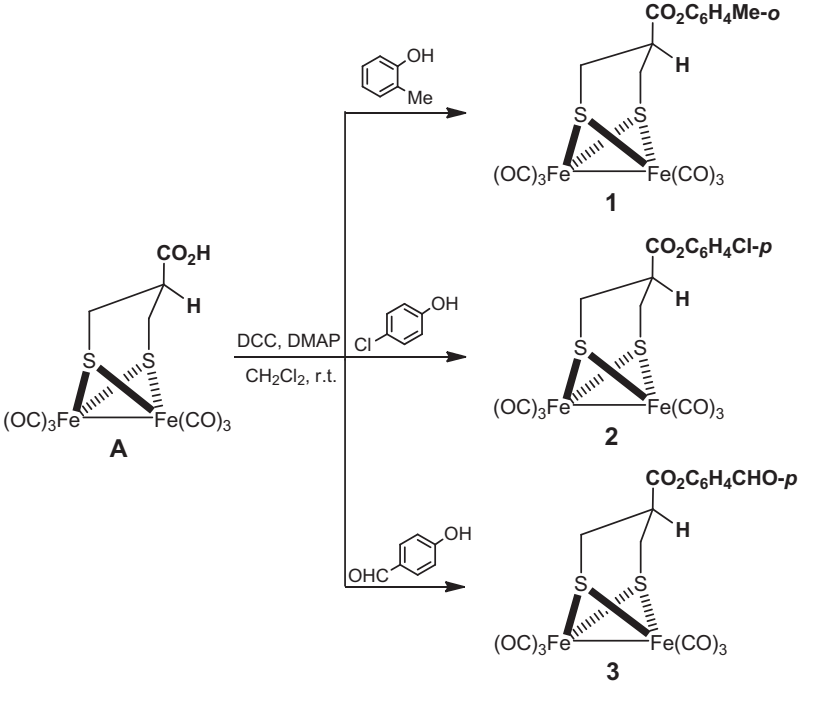

Scheme 1. Preparation of **1–3**.

4. Conclusion

As active site mimics of [FeFe]-hydrogenase, three new bridgehead-C-functionalized diiron dithiolate complexes **1–3** can be prepared by condensation reactions of $[(\mu\text{-}SCH_2)_2CHCO_2H][Fe_2(CO)_6]$ (**A**) with *o*-MeC_6H_4OH, *p*-ClC_6H_4OH, or *p*-HOC_6H_4CHO in the presence of the dehydrating reagent DCC and the catalyst DMAP in CH_2Cl_2 at room temperature. **1–3** were structurally characterized by elemental analysis, spectroscopy, and X-ray crystallography. Complex **1** is an electrocatalyst for proton reduction to H_2 in the presence of HOAc. From spectroscopic, crystallographic, and electrochemical studies on **1–3**, the bridgehead (X) functionality of PDT bridge (SCH_2XCH_2S) in this kind of diiron carbonyl complexes exerts little influence on the molecular geometries and electrocatalytic behaviors of the corresponding diiron dithiolate model complexes.

Supplementary material

CCDC-987203 (**1**), CCDC-987204 (**2**), and CCDC-987206 (**3**) contain the supplementary crystallographic data for this article. These data can be obtained free of charge via http://www.ccdc.cam.ac.uk/conts/retrieving.html, or from the Cambridge Crystallographic Data Center, 12 Union Road, Cambridge CB2 1EZ, UK; Fax: (+44) 1223 336 033; or Email: deposit@ccdc.cam.ac.uk.

Funding

This work was financially supported by the National Natural Science Foundation of China [grant number 21301160]; the Natural Science Foundation for Young Scholars of Shanxi Province [grant number 2012021007-4].

References

[1] J. Alper. *Science*, **299**, 1686 (2003).
[2] W. Lubitz, W. Tumas. *Chem. Rev.*, **107**, 3900 (2007).
[3] J.W. Peters, W.N. Lanzilotta, B.J. Lemon, L.C. Seefeldt. *Science*, **282**, 1853 (1998).
[4] Y. Nicolet, C. Piras, P. Legrand, C.E. Hatchikian, J.C. Fontecilla-Camps. *Structure*, **7**, 13 (1999).
[5] A. Le Cloirec, S.P. Best, S.C. Davies, D.J. Evans, D.L. Hughes, C.J. Pickett. *Chem. Commun.*, **1999**, 2285 (1999).
[6] G. Berggren, A. Adamska, C. Lambertz, T.R. Simmons, J. Esselborn, M. Atta, S. Gambarelli, J.M. Mouesca, E. Reijerse, W. Lubitz, T. Happe, V. Artero, M. Fontecave. *Nature*, **499**, 66 (2013).
[7] R.D. Bethel, M.Y. Darensbourg. *Nature*, **499**, 40 (2013).
[8] J.-X. Jian, Q. Liu, Z.-J. Li, F. Wang, X.-B. Li, C.-B. Li, B. Liu, Q.-Y. Meng, B. Chen, K. Feng, C.-H. Tung, L.-Z. Wu. *Nat. Commun.*, **4**, 3695 (2013).
[9] J.-F. Capon, F. Gloaguen, P. Schollhammer, J. Talarmin. *Coord. Chem. Rev.*, **249**, 1664 (2005).
[10] C. Tard, C.J. Pickett. *Chem. Rev.*, **109**, 2245 (2009).
[11] F. Gloaguen, T.B. Rauchfuss. *Chem. Soc. Rev.*, **38**, 100 (2009).
[12] M. Fontecave, V. Artero. *C. R. Chimie*, **14**, 362 (2011).
[13] M.Y. Darensbourg, W. Weigand. *Eur. J. Inorg. Chem.*, **2011**, 994 (2011).
[14] B.-S. Yin, T.-B. Li, M.-S. Yang. *J. Coord. Chem.*, **64**, 2066 (2011).
[15] C.A. Mebi, D.S. Karr, R.X. Gao. *J. Coord. Chem.*, **64**, 4397 (2011).
[16] X.-F. Liu, W.-X. Xiao, L.-J. Shen. *J. Coord. Chem.*, **64**, 1023 (2011).
[17] S. Salyi, M. Kritikos, B. Åkermark, L. Sun. *Chem. Eur. J.*, **9**, 557 (2003).
[18] C.M. Thomas, O. Rüdiger, T.-B. Liu, C.E. Carson, M.B. Hall, M.Y. Darensbourg. *Organometallics*, **26**, 3976 (2007).

[19] L.-C. Song, C.-G. Li, J. Gao, B.-S. Yin, X. Luo, X.-G. Zhang, H.-L. Bao, Q.-M. Hu. *Inorg. Chem.*, **47**, 4545 (2008).
[20] L.-C. Song, X.-F. Liu, J.-B. Ming, J.-H. Ge, Z.-J. Xie, Q.-M. Hu. *Organometallics*, **29**, 610 (2010).
[21] U.-P. Apfel, C.R. Kowol, F. Kloss, H. Görls, B.K. Keppler, W. Weigand. *J. Organomet. Chem.*, **696**, 1084 (2011).
[22] L.-C. Song, W. Gao, X. Luo, Z.-X. Wang, X.-J. Sun, H.-B. Song. *Organometallics*, **31**, 3324 (2012).
[23] C.-G. Li, Y. Zhu, X.-X. Jiao, X.-Q. Fu. *Polyhedron*, **67**, 416 (2014).
[24] P.-H. Zhao, Y.-Q. Liu, G.-Z. Zhao. *Polyhedron*, **53**, 144 (2013).
[25] P.-H. Zhao, X.-H. Li, Y.-F. Liu, Y.-Q. Liu. *J. Coord. Chem.*, **67**, 766 (2014).
[26] P.-H. Zhao, Y.-F. Liu, K.-K. Xiong, Y.-Q. Liu. *J. Cluster Sci.*, **25**, 1061 (2014).
[27] P.-H. Zhao, S.-N. Liu, Y.-F. Liu, Y.-Q. Liu. *J. Cluster Sci.*, **25**, 1331 (2014).
[28] P.-H. Zhao, W.-T. Wang, Y.-F. Liu, Y.-Q. Liu. *Transition Met. Chem.*, **39**, 501 (2014).
[29] L.-C. Song, P.-H. Zhao, Z.-Q. Du, M.-Y. Tang, Q.-M. Hu. *Organometallics*, **29**, 5751 (2010).
[30] L.-C. Song, X.-J. Sun, P.-H. Zhao, J.-P. Li, H.-B. Song. *Dalton Trans.*, **41**, 8941 (2012).
[31] *CRYSTALCLEAR 1.3.6*, Rigaku and Rigaku/MSC, The Woodlands, TX (2005).
[32] G.M. Sheldrick. *SHELXS97, A Program for Crystal Structure Solution*, University of Göttingen, Germany (1997).
[33] G.M. Sheldrick. *SHELXL97, A Program for Crystal Structure Refinement*, University of Göttingen, Germany (1997).
[34] S.D. Gong, C.Y. Wang, Q.-S. Li, Y.M. Xie, R.B. King. *J. Coord. Chem.*, **65**, 2459 (2012).
[35] Y.-C. Shi, W. Yang, Y. Shi, D.-C. Cheng. *J. Coord. Chem.*, **67**, 2330 (2014).
[36] X.-F. Liu, M.-Y. Chen, H.-Q. Gao. *J. Coord. Chem.*, **67**, 57 (2014).
[37] P.I. Volkers, T.B. Rauchfuss, S.R. Wilson. *Eur. J. Inorg. Chem.*, **2006**, 4793 (2006).
[38] R. Mejia-Rodriguez, D. Chong, J.H. Reibenspies, M.P. Soriaga, M.Y. Darensbourg. *J. Am. Chem. Soc.*, **126**, 12004 (2004).
[39] J.F. Capon, F. Gloaguen, F.Y. Pétillon, P. Schollhammer, J. Talarmin. *Coord. Chem. Rev.*, **253**, 1476 (2009).
[40] G.A.N. Felton, C.A. Mebi, B.J. Petro, A.K. Vannucci, D.H. Evans, R.S. Glass, D.L. Lichtenberger. *J. Organomet. Chem.*, **694**, 2681 (2009).